

RESEARCH ARTICLE

Editorial Process: Submission:05/02/2025 Acceptance:01/08/2026 Published:01/21/2026

Monte Carlo Investigation of Field Size Effects on Central-Axis Dose Distributions (PDD Curves) and Lateral Dose Profiles**Elsayed M. Alashkar*, Ahmed A. Abdel-Aal, Ayman S. El Shinawy, M. A. Abu Ghazala, Hussein M. Abdelhafez****Abstract**

Introduction: After radioactivity and X-rays were first discovered, researchers found that radiation could harm cells by damaging their internal structures, with cancer cells particularly vulnerable to these effects. Today, various advanced machines and methods are employed to enhance the precision of radiation delivery to tumors. Monte Carlo simulation is an excellent method for predict the dose distributions under certain conditions. Therefore, in this study, we aimed to investigate the field size effect on the central dose distributions (PDD Curves), and the lateral profiles of the dose. **Method:** MC codes, i)- MCBEAM code, ii)- MCSIM code, and iii) MCSHOW code used to simulate 6MV photon beams with 5 different field sizes (10x10cm, 5x5cm, 8x8cm, 15x15cm, and 20x20cm). PDDs and profile curves were compared for each field size. **Result:** Smaller field sizes (e.g., 5x5 cm) exhibited a lower surface dose compared to larger fields, and the depth of maximum dose d_{max} shifts slightly deeper as field size increases due to increased scatter contributions. Larger fields (15x15 cm, 20x20 cm) demonstrated a slower dose falloff at deeper depths compared to smaller fields. **Conclusion:** Monte Carlo calculations confirms that field size significantly impacts PDD curves and affects surface dose. This agreement encouraged us to research with these codes to improve treatment techniques in radiotherapy.

Keywords: Beam modeling- Beam simulation- Dose profile- Monte Carlo simulation- PDD curve

Asian Pac J Cancer Prev, 27 (1), 123-128

Introduction

High-energy radiation can disrupt cellular structures, which is the fundamental principle behind radiotherapy [1]. Early X-ray generators in the 1920s were limited to producing 200 kV X-rays, whereas modern linear accelerators generate X-rays in the megavolt range [2]. Radiotherapy is often combined with surgery, chemotherapy, and biological therapy to treat, manage, or alleviate cancer symptoms. It is the second most common and effective cancer treatment after surgery, used in over 50% of cancer cases [3].

The primary objective of radiotherapy is to administer a lethal dose to tumor cells while sparing surrounding healthy tissues. However, this is challenging because tumors are frequently situated near radiosensitive organs like the brain stem, spinal cord, lungs, or intestines, known as Organs at Risk (OARs), which must be protected during treatment [4].

Over time, advanced radiotherapy techniques such as IMRT, DE, MERT, eARC, and VMAT have been developed, each with specific parameters that influence treatment precision [5]. Since directly measuring dose distribution in patients is rarely feasible, most data are

obtained from tissue-equivalent phantoms that mimic full-scatter conditions. These measurements are then used in computational models to predict dose distribution in actual patients [6].

Water phantoms are commonly used for dose calibration because their radiation absorption and scattering properties closely resemble human soft tissues. Additionally, water is widely available and has consistent radiation characteristics [7, 8]. The absorbed dose in a patient (or phantom) varies with depth, influenced by factors such as beam energy, field size, source distance, and collimation. A critical aspect of dose calculation is determining the depth-dose variation along the beam's central axis [9].

Monte Carlo (MC) simulation is the gold standard for modeling radiation transport, making it invaluable for radiotherapy research, particularly in developing new techniques. Accurate modeling of linear accelerator components is essential for reliable simulations [10]. For instance, Lee et al. [11] investigated multi-leaf collimated electron beams for MERT using both MC simulations and experimental methods.

Monte Carlo methods, dating back over two centuries, are widely used for solving complex mathematical

problems, such as numerical integration. These simulations rely on pseudo-random numbers generated by algorithms, allowing approximations with finite sampling. MC methods are particularly useful in high-dimensional problems, such as calculating radiation dose distributions in patients, where solving the transport equation is necessary [12].

The transport equation varies per patient and depends on treatment parameters like beam energy, direction, and field size. MC simulations solve this equation by tracking individual particle histories recording each photon or electron's path until its energy is fully absorbed or it exits the region of interest. Interactions with tissue, including energy loss and secondary particle production, are governed by probability distributions derived from cross-section data [13].

Significant efforts have been made to integrate MC dose engines into treatment planning systems. One approach involves adapting general-purpose MC codes like EGS4/EGSnrc for clinical use [14]. Alternatively, specialized MC algorithms such as VMC (for electrons) and XVMC (for photons) have been developed, enabling rapid dose calculations on standard computers [15].

Currently, many treatment planning systems are incorporating MC-based dose calculations, with some already in clinical use. In the future, MC methods are expected to replace conventional dose algorithms entirely.

Materials and Methods

A-Instrumentation: MC codes which are used in the present work are: i)- MCBEAM code, ii)- MCSIM code, iii) MCSHOW code.

MCBEAM approach

The MCBEAM method is an EGS4/PRESTA-based computational tool designed for simulating high-energy electron and photon beams from medical

linear accelerators. Developed primarily for educational and research purposes, this approach incorporates fundamental geometric components such as SLABS, CONES, BLOCKS, JAWS, and FRAMES which are modular, reusable, and can be combined to model various accelerator configurations.

The system supports multiple source inputs, including a frontal point source with adjustable polar angle limits, a frontal parallel source, and a phase-space source. Only two essential files are required: the PEGS4 file (containing cross-section data), and the user input file (defining accelerator geometry, beam parameters, and output specifications). Once compiled, MCBEAM can simulate different accelerator models without recompilation. Users simply modify the input file for new configurations. Additionally, particle trajectories can be tracked and recorded at multiple planes (at various points along the treatment head) and saved in phase-space files for further analysis.

The treatment head is a thick shield made of an alloy of tungsten and lead to protect its components and to absorb X-rays from all directions except in the direction of the fixed collimator (the forward direction of the beam). The head contains according to Figure 1, the following: 1- The target: at which the X-rays are produced; it can be removed, if we need to use the accelerator in the electron mode. 2- The electron scattering foil. 3- Flattening filters. 4- Ionization chambers. 5- Fixed and movable collimators.

MCSIM approach

The MCSIM approach was developed as a Monte Carlo-based computational tool for radiotherapy dose calculations and treatment verification. Built upon the EGS4 framework, this method provides independent dose verification for conventional photon and electron treatments, as well as advanced techniques like modulated electron radiotherapy (MERT) and intensity-modulated radiation therapy (IMRT). One of its key advantages is the

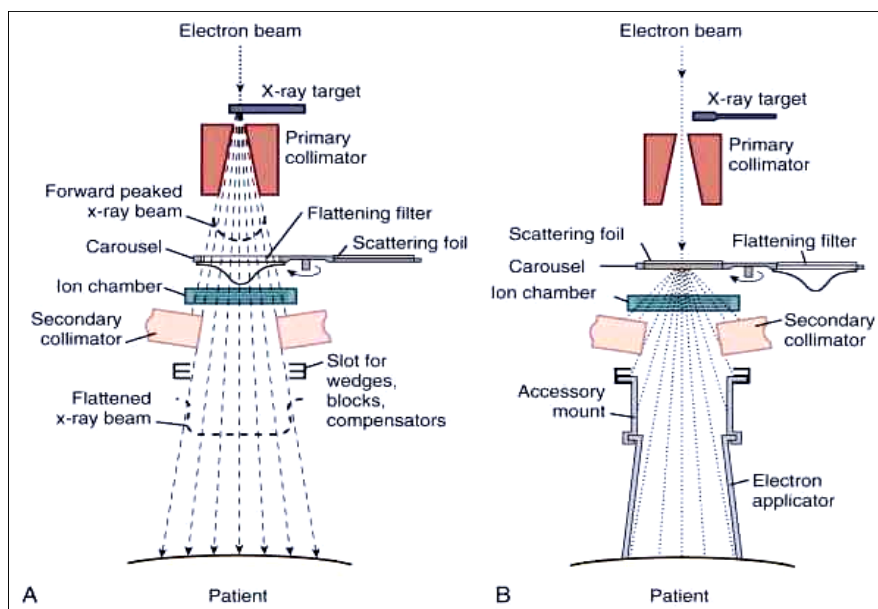


Figure 1. Schematic Illustrations of the Key Treatment Head Components in a Varian Linear Accelerator. (A) Configuration for X-ray therapy. (B) Setup for electron therapy.

ability to investigate novel treatment techniques not yet available in commercial systems. Additionally, it serves as a valuable tool for verifying treatment planning system (TPS) results either before or after treatment delivery and enables clinical research on cases beyond the capabilities of existing TPS software.

The system allows users to define simulation geometry through manual input of voxel dimensions, material types, and mass densities, all specified in a dedicated MCSIM input file along with parameters for beam modifiers. For dose analysis, the companion program MCSHOW enables visualization and comparison of isodose distributions and dose-volume histograms (DVHs). The simulation performs full particle transport for various beam modifiers including jaws, wedges, compensators, blocks, and electron cutouts. It can model bolus effects by incorporating the bolus material directly into patient geometry and simulates both static MLC fields (approximated through blocks) and dynamic MLC/wedge configurations.

MCSIM offers several advanced features, including the capability to simulate multiple gantry angles in a single run and a built-in function to convert CT numbers (or electron density values) to appropriate materials and mass densities using the Phantom Creator code. The system employs similar multiple source models for both photon and electron beams, with photon beam phase-space parameters being reconstructable at any user-defined plane perpendicular to the central axis.

The simulation utilizes standard EGS4 transport parameters, which include energy thresholds for secondary particle creation (AE, AP), energy cutoffs for particle transport (ECUT, PCUT), and electron step controls (SMAX, ESTEPE). Notably, when simulating phantoms with large voxels or high-Z materials, users can input smaller ESTEPE values (such as 0.04 or 0.01) to improve accuracy, though this increases computation time due to the greater number of scattering steps required. Several variance reduction techniques are implemented in MCSIM, including photon interaction forcing, Russian roulette, electron range/region rejection, and correlated sampling (electron track repeating), all of which can be selectively enabled or disabled during patient dose calculations depending on the specific requirements of the simulation.

MCSHOW program

The MCSIM simulation generates its output as 3D DOSE files, which contain comprehensive dose distribution data. These files can be processed and visualized using the dedicated MCSHOW program, a specialized Monte Carlo graphical interface tool. MCSHOW offers multiple analytical functions to characterize radiation beam properties, including the generation of Percentage Depth Dose (PDD) curves along the beam's central axis and Dose Profiles representing lateral dose distributions at various depths within the phantom. This capability allows for a detailed examination of dosimetric parameters at any selected depth from the phantom surface.

B- Procedure

The MCBEAM method, as previously described, models the treatment head of Varian linear accelerators to generate precise photon beam phase space data. This simulation incorporates the exact dimensions and material compositions of accelerator components based on manufacturer specifications. For electron transport, energy cutoffs (ECUT and AE) are set at 700 keV (total energy), while photon transport parameters (PCUT and AP) use a 10 keV threshold. The simulation limits electron step length to ensure maximum energy loss per step does not exceed 4% (ESTEPE = 0.04), employing ICRU [16] recommended stopping power values for various materials. Air gaps along the particle transport path are explicitly modeled. The resulting phase space data from MCBEAM serves as the radiation source input for subsequent MCSIM dose calculations in water phantoms, maintaining identical transport parameters (ECUT, AE, PCUT, AP, and ESTEPE). MCPLAN then simulates treatment delivery, incorporating jaws, pMLC, and electron cutouts as beam modifiers within either 3D patient anatomy or phantom geometries.

This investigation proceeded through five main steps

(i) Monte Carlo modeling of the head machine components (by MCBEAM approach). We calculated phase-space files for 5 different photon beams, each of them with energy of 6 MV.

The calculated photon beams with 5 different field sizes, which were 10x10cm, 5x5cm, 8x8cm, 15x15cm, and 20x20cm, respectively.

10x10cm field size is the reference field size in radiotherapy. The two field size groups, which consist of 5x5cm and 8x8cm field sizes, are two field sizes smaller than the reference field size, where the group of two field sizes 15x15cm, and 20x20cm, represent the groups of largest field sizes than the reference field size. We chose these values of the field sizes to study the effect of field size around the value of the reference field size itself (smaller and larger, both sides)

(ii) Monte Carlo simulation (by MCSIM approach): continue to calculate the resulted phase-space files in the water phantom, with the same physical parameters of 6MV energy and the 5 different field sizes (10x10cm, 5x5cm, 8x8cm, 15x15cm, and 20x20cm). Each field size was calculated in the water phantom to consist of Voxels with $0.1 \times 0.1 \times 0.1 \text{ cm}^3$ dimensions.

(iii) MCSHOW program: used to show the final form and the result of the dose distributions of each field size, the dose distribution displayed in two planes (Vertical and horizontal planes), we export the PDD curve for each field size, and export beam profiles for each field size (export 5 profile at different depths, 1.5cm, 3cm, 5cm, 10cm, and 15cm, respectively).

(iv) Analyze how dose distribution varies with field size by plotting percentage depth dose (PDD) curves for each field size and comparing them across different field dimensions.

(v) Compare the dose distribution variation with the field size effect across the fields and draw their curves (profiles curves).

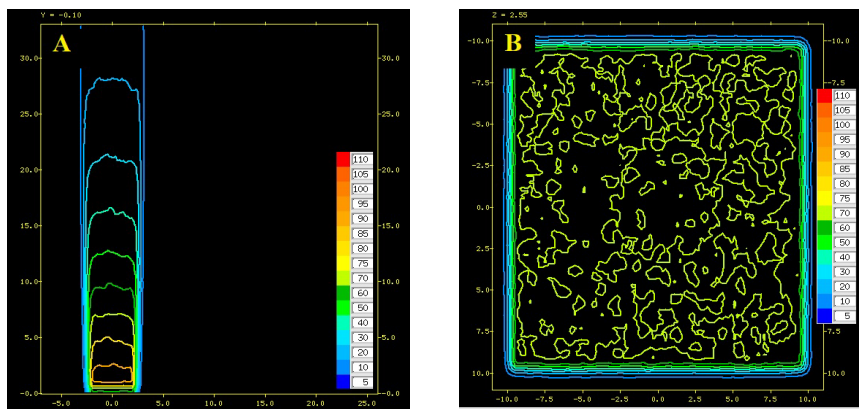


Figure 2. Dose Distribution Patterns and Isodose Lines from a 6 Million Volt Photon beam 10×10 cm² (Reference Field Size), in Water Phantom, Showing (A) vertical and (B) horizontal planes.

Results

Monte Carlo simulations for 6MV photon beams yielded the following outcomes:

1- The first section displays the dose distributions and isodose lines were generated for both vertical and horizontal planes across five field sizes (10×10 cm², 5×5 cm², 8×8 cm², 15×15 cm², and 20×20 cm²), as illustrated in Figures 2 through 6 respectively.

2- The second section displays dose distribution curves, including Percentage Depth Dose (PDD) along the central axis and cross-beam profiles calculated at five depths (1.5 cm, 3 cm, 5 cm, 10 cm, and 15 cm), for all field sizes (10×10 cm², 5×5 cm², 8×8 cm², 15×15 cm², and 20×20 cm²). This displayed in Supplementary Figures 1- 5.

3- The Third section presents the comparison between calculated Percentage Depth Dose (PDD) curves, across all investigated field sizes (10×10 cm², 5×5 cm²,

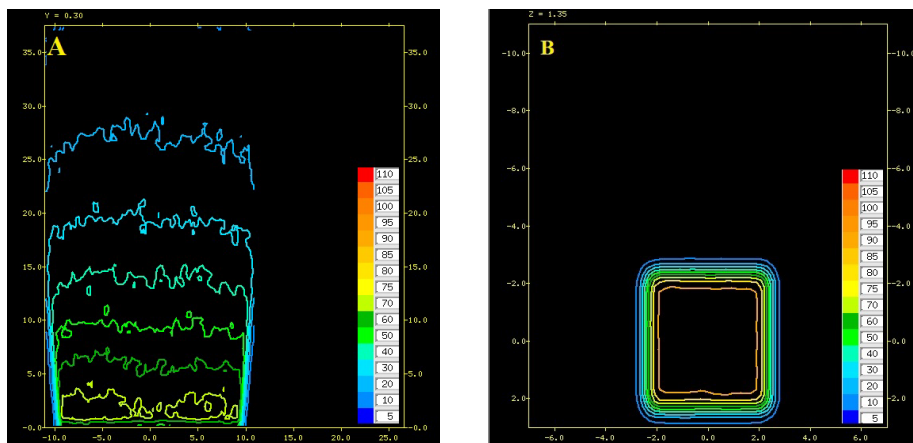


Figure 3. Dose Distribution Patterns and Isodose Lines from a 6 Million Volt Photon beam 5×5 cm² Field Size, in Water Phantom, Showing (A) vertical and (B) horizontal planes.

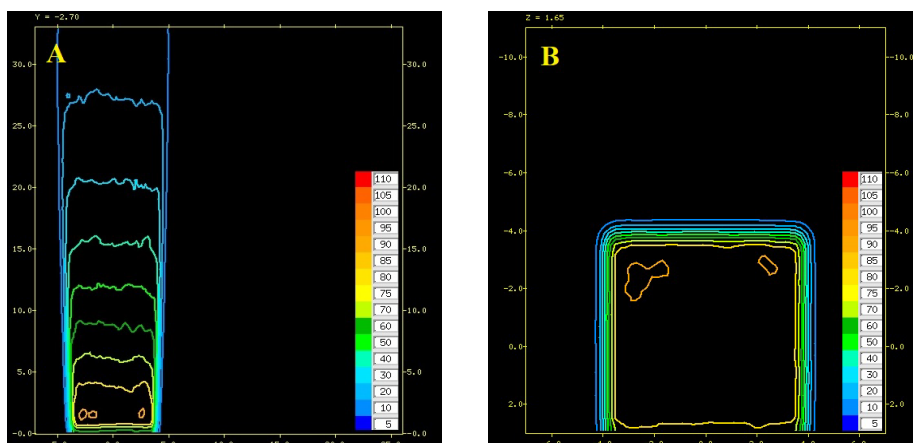


Figure 4. Dose Distribution Patterns and Isodose Lines from a 6 Million Volt Photon beam 8×8 cm² Field Size, in Water Phantom, Showing (A) vertical and (B) horizontal planes.

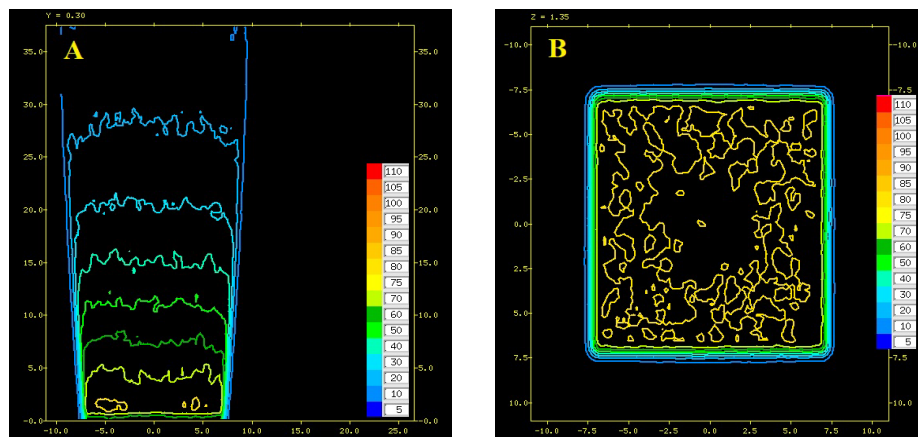


Figure 5. Dose Distribution Patterns and Isodose Lines from a 6 Million Volt Photon Beam 15×15 cm² Field Size, in Water Phantom, Showing (A) vertical and (B) horizontal planes.

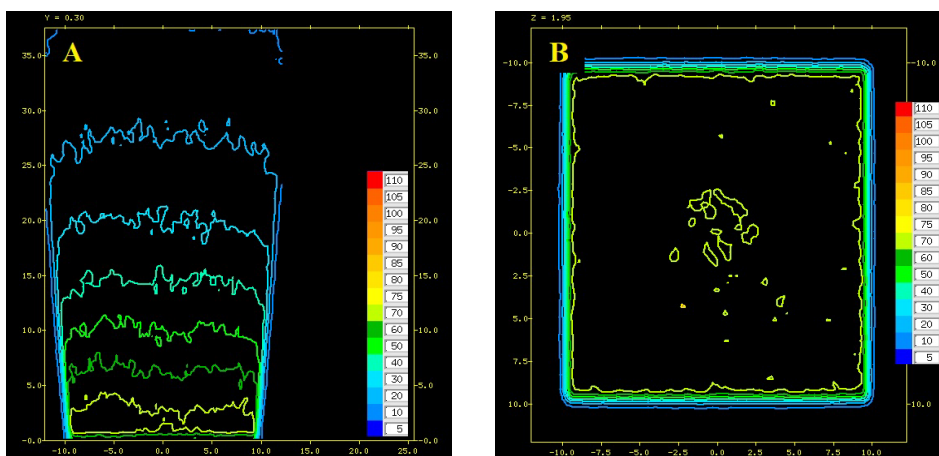


Figure 6. Dose Distribution Patterns and Isodose Lines from a 6 Million Volt Photon beam 20×20 cm² Field Size, in Water Phantom, Showing (A) vertical and (B) horizontal planes.

8×8 cm², 15×15 cm², and 20×20 cm²), as presented in Supplementary Figure 6.

Discussion

The Percentage Depth Dose (PDD) describes how radiation dose is deposited at different depths along the central axis in a medium (typically water or tissue) for a given beam energy and field size [17].

In this analysis, we compare calculated PDD curves for radiation beam of 6MV photon energy with 5 different field sizes (10×10 cm, 5×5 cm, 8×8 cm, 15×15 cm, and 20×20 cm), as displayed in Figure 12. We observed that the smaller field sizes (5×5 cm) exhibit a lower surface dose compared to larger fields (20×20 cm). This may be because larger fields have more scattered radiation contributing to dose buildup near the surface [18].

Also, we noticed that the Depth of Maximum Dose (d_{max}) shifts slightly deeper as field size increases due to increased scatter contributions. For a 6 MV photon beam, d_{max} may be ~1.5 cm for 5×5 cm but ~2.0 cm for 20×20 cm. Larger fields (15×15 cm, 20×20 cm) showed a slower dose falloff at deeper depths compared to smaller fields. Increased scatter from a larger irradiated volume contributes to the dose at depth [19].

Based on our findings, the smaller fields (5×5 cm, 8×8 cm) may be better for superficial lesions treatment (less skin sparing needed), [20]. Also, Faster dose falloff helps spare deeper tissues (e.g., spinal cord in spine SBRT), [21]. Medium fields (10×10 cm) are standard reference for most treatments (balanced scatter and penetration), [22]. Larger fields (15×15 cm, 20×20 cm) are useful for whole breast, pelvic, or abdominal treatments but higher surface doses may increase skin reactions [23]. Slower falloff means more doses to deeper organs (e.g., rectum in prostate RT), [24].

In conclusion, field size significantly impacts PDD curves and beam profiles, affecting surface dose, d_{max}, and depth dose distribution. Larger fields have higher surface dose, deeper d_{max}, and slower falloff due to increased scatter. Smaller fields are preferable when deep tissue sparing is critical. The strong agreement between Monte Carlo calculations and experimentally measured dose distributions confirms its status as an indispensable tool in radiotherapy studies. Continued refinement of these simulations will drive innovation in therapeutic approaches and techniques.

Author Contribution Statement

All authors contributed equally in this study.

Acknowledgements

None.

References

1. Majeed H, Gupta V. Adverse Effects of Radiation Therapy. [Updated 2023 Aug 14]. In: StatPearls [Internet]. Treasure Island (FL): StatPearls Publishing; 2025 Jan. Available from:<https://www.ncbi.nlm.nih.gov/books/NBK563259/>
2. Cunningham JR, Johns HE. The physics of radiology. Lawrence avenue, springfield, illinois, USA: Charles tomas; 227-501.
3. Khan MK, Nasti TH, Buchwald ZS, Weichselbaum RR, Kron SJ. Repurposing drugs for cancer radiotherapy: Early successes and emerging opportunities. *Cancer J.* 2019;25(2):106-15. <https://doi.org/10.1097/ppo.0000000000000369>.
4. Kirthi Koushik AS, Harish K, Avinash HU. Principles of radiation oncology: A beams eye view for a surgeon. *Indian J Surg Oncol.* 2013;4(3):255-62. <https://doi.org/10.1007/s13193-013-0231-1>.
5. Rana S. Intensity modulated radiation therapy versus volumetric intensity modulated arc therapy. *J Med Radiat Sci.* 2013;60(3):81-3. <https://doi.org/10.1002/jmrs.19>.
6. Pimenta EB, Nogueira LB, de Campos TPR. Dose measurements in a thorax phantom at 3dert breast radiation therapy. *Rep Pract Oncol Radiother.* 2021;26(2):242-50. <https://doi.org/10.5603/RPOR.a2021.0037>.
7. Arjunan M, Sekaran SC, Sarkar B, Manikandan S. A homogeneous water-equivalent anthropomorphic phantom for dosimetric verification of radiotherapy plans. *J Med Phys.* 2018;43(2):100-5. https://doi.org/10.4103/jmp.JMP_123_17.
8. Zuber SH, Hadi M, Samson DO, Jayamani J, Rabaei NA, Aziz MZA, et al. Dosimetric analysis of rhizophora-based phantom material in radiation therapy applications using monte carlo gate simulation. *J Med Phys.* 2023;48(4):358-64. https://doi.org/10.4103/jmp.jmp_75_23.
9. Bencheikh M, Maghnouj A, Tajmouati J. Dosimetry quality control based on percent depth dose rate variation for checking beam quality in radiotherapy. *Rep Pract Oncol Radiother.* 2020;25(4):484-8. <https://doi.org/10.1016/j.rpor.2020.03.016>.
10. Shende R, Dhoble SJ, Gupta G. Dosimetric evaluation of radiation treatment planning for simultaneous integrated boost technique using monte carlo simulation. *J Med Phys.* 2023;48(3):298-306. https://doi.org/10.4103/jmp.jmp_4_23.
11. Lee MC, Jiang SB, Ma CM. Monte Carlo and experimental investigations of multileaf collimated electron beams for modulated electron radiation therapy. *Medical physics.* 2000 Dec;27(12):2708-18.
12. Cirauqui D, Garcia-March MA, Corominas G, Grass T, Grzybowski P, Muñoz-Gil G, et al. Comparing pseudo- and quantum-random number generators with monte carlo simulations. *APL Quantum.* 2024;1. <https://doi.org/10.1063/5.0199568>.
13. Liang Y, Muhammad W, Hart GR, Nartowt BJ, Chen ZJ, Yu JB, et al. A general-purpose monte carlo particle transport code based on inverse transform sampling for radiotherapy dose calculation. *Sci Rep.* 2020;10(1):9808. <https://doi.org/10.1038/s41598-020-66844-7>.
14. Park H, Paganetti H, Schuemann J, Jia X, Min CH. Monte carlo methods for device simulations in radiation therapy. *Phys Med Biol.* 2021;66(18). <https://doi.org/10.1088/1361-6560/ac1d1f>.
15. Kawrakow I. Accurate condensed history monte carlo simulation of electron transport. I. Egsnc, the new egs4 version. *Medical Physics.* 2000;27(3):485-98. <https://doi.org/10.1118/1.598917>.
16. ICRU. Stopping Powers and Ranges for Electrons and Positrons. ICRU Report 37. International Commission on Radiation Units and Measurements, Bethesda, Md;1984.
17. Khan FM. "The physics of radiation therapy", Williams and Wilkins, Baltimore, Maryland, U.S.A.1994.
18. Sigamani A, Nambiraj A, Yadav G, Giribabu A, Srinivasan K, Gurusamy V, et al. Surface dose measurements and comparison of unflattened and flattened photon beams. *J Med Phys.* 2016;41(2):85-91. <https://doi.org/10.4103/0971-6203.181648>.
19. Mott JHL, West NS. Essentials of depth dose calculations for clinical oncologists. *Clin Oncol (R Coll Radiol).* 2021;33(1):5-11. <https://doi.org/10.1016/j.clon.2020.06.021>.
20. Seif F, Bayatian MR. Evaluation of electron contamination in cancer treatment with megavoltage photon beams: Monte carlo study. *J Biomed Phys Eng.* 2015;5(1):31-8.
21. Tseng CL, Eppinga W, Charest-Morin R, Soliman H, Myrehaug S, Maralani PJ, et al. Spine stereotactic body radiotherapy: Indications, outcomes, and points of caution. *Global Spine J.* 2017;7(2):179-97. <https://doi.org/10.1177/2192568217694016>.
22. Fogliata A, Stravato A, Reggiori G, Tomatis S, Würfel J, Scorsetti M, et al. Collimator scatter factor: Monte carlo and in-air measurements approaches. *Radiat Oncol.* 2018;13(1):126. <https://doi.org/10.1186/s13014-018-1070-6>.
23. Bahreyni Toossi MT, Mohamadian N, Mohammadi M, Ghorbani M, Hassani M, Khajetash B, et al. Assessment of skin dose in breast cancer radiotherapy: On-phantom measurement and monte carlo simulation. *Rep Pract Oncol Radiother.* 2020;25(3):456-61. <https://doi.org/10.1016/j.rpor.2020.03.008>.
24. Shah SH, Gupta AK. Protection of the rectum during prostate radiation. *Semin Intervent Radiol.* 2020;37(3):324-9. <https://doi.org/10.1055/s-0040-1713449>.



This work is licensed under a Creative Commons Attribution-Non Commercial 4.0 International License.